

ELEMENT: Episodic and Lifelong Exploration via Maximum Entropy

Hongming Li, Shujian Yu, Bin Liu, José C. Príncipe *Life Fellow, IEEE*,

Abstract—This paper proposes *Episodic and Lifelong Exploration via Maximum ENTropy* (ELEMENT), a novel, multiscale, intrinsically motivated reinforcement learning (RL) framework that is able to explore environments without using any extrinsic reward and transfer effectively the learned skills to downstream tasks. We advance the state of the art in three ways. First, we propose a multiscale entropy optimization to take care of the fact that previous maximum state entropy, for lifelong exploration with millions of state observations, suffers from vanishing rewards and becomes very expensive computationally across iterations. Therefore, we add an episodic maximum entropy over each episode to speedup the search further. Second, we propose a novel intrinsic reward for episodic entropy maximization named *average episodic state entropy* which provides the optimal solution for a theoretical upper bound of the episodic state entropy objective. Third, to speed the lifelong entropy maximization, we propose a k nearest neighbors (k NN) graph to organize the estimation of the entropy and updating processes that reduces the computation substantially. Our ELEMENT significantly outperforms state-of-the-art intrinsic rewards in both episodic and lifelong setups. Moreover, it can be exploited in task-agnostic pre-training, collecting data for offline reinforcement learning, etc.

Index Terms—Reinforcement Learning for Exploration, Maximum Entropy, Intrinsic Learning

I. INTRODUCTION

Reinforcement Learning (RL) has achieved remarkable success in fields like robotics [1] and games [2]. Nonetheless, its practical applications in real-world scenarios are still restricted due to the high variability and lack of user control on the density of rewards, which are critical for sample efficiency and success of RL. To counteract this shortcoming, intrinsically motivated exploration [3] has been put forth to encourage the agent to explore unknown states in the absence of extrinsic rewards, by offering an intrinsic reward.

Recently, the state entropy $H(s)$ serves as a well-defined quantity to measure the diversity of state visitations, making it a popular intrinsic reward for exploration [4, 5, 6, 7] and various sampling methods [8, 9, 10, 11, 12]. For non-tabular state entropy maximization, Liu et.al [4] propose a popular method to estimate state entropy by measuring distances between states and their k -nearest neighbors, a.k.a., Kozachenko-Leonenko k NN entropy estimator [13]. However, these distance-based methods [4, 6, 7] face a fundamental

limitation due to the vanishing trend of lifelong rewards: after a state has been visited, its novelty/reward vanishes drastically, and then the agent is not encouraged to revisit it, regardless of the potential downstream exploration opportunities it might allow [14, 15, 16, 17]. This approach diminishes the likelihood of exploring further regions via similar routes because the lifelong rewards on these paths decrease rapidly.

To overcome this issue, we offer an elegant solution by incorporating an episodic exploration mechanism [16] under the motivation that episodic setting encourages an agent to revisit familiar (but not fully explored) states over recent episodes [17]. Our approach, termed **ELEMENT**, aims to jointly fostering Episodic and Life-long Exploration under the Maximum ENTropy principle. Maximizing lifelong state entropy across all historically visited states slowly discourages revisits to frequently visited states over all episodes. Conversely, maximizing episodic state entropy quickly discourages revisiting the same state within a single episode.

Albeit the simplicity of our idea, implementing ELEMENT is a non-trivial task. One reason is that the state entropy in an episode provides one single trajectory-wise bonus only at the conclusion of each long-term episode, which is a Partially Observed Markovian decision process (POMDP). In contrast, standard RLs learn by exploiting dense Markovian rewards for each state in episodes. To solve this problem, we propose a novel intrinsic reward termed *average episodic state entropy*, which is a Markovian proxy reward function, offering a theoretically grounded sub-optimal solution. This strategy enables the usage of any entropy estimator in the episodic exploration, but is infeasible for the lifelong state entropy maximization due to the computational complexity burden which escalates as the number of visited states grows. To this end, we further identified that popular entropy estimators, such as kernel density estimator, k -nearest neighbors (k NN) estimator [13] and matrix-based Rényi's entropy functional estimator [18], are essentially (approximately) proportional to a sum decomposition based on k NN distances. This motivates us to leverage a fast k NN graph to make these estimator practical in lifelong exploration, by integrating a modified greedy graph search algorithm [19] with an online updating mechanism [20]. To summarize, our main contributions include:

- We propose a novel intrinsically motivated policy learning method for joint **Episodic and Life-long Exploration** using **Maximum ENTropy** principle (ELEMENT), which resides on the multi-scale entropy estimation to derive internal rewards for pure exploration in RL.
- To address the POMDP challenge inherent in maximizing episodic entropy, we propose a theoretically grounded

Corresponding to Shujian Yu (yusj9011@gmail.com) and Bin Liu (bins@ieee.org)

Hongming Li is with the Zhejiang Lab, Huangzhou, China. Shujian Yu is with the Vrije Universiteit Amsterdam, Amsterdam, the Netherlands. Bin Liu is with Tianyi Digital Life Technology Co. Ltd. José C. Príncipe is with Computational NeuroEngineering Laboratory at the University of Florida, Gainesville, USA

standard Markovian reward function which assigns larger rewards to states consistently appear in high-entropy episodes. To speed the lifelong entropy maximization, we propose a k NN graph to organize the estimation of the entropy.

- ELEMENT is compared with four state-of-the-art (SOTA) intrinsic rewards, such as NGU [17] and RISE [7], in five exploration environments. It outperforms all competing approaches in experiments including episodic state entropy maximization, exploring novel states, collecting data for offline RL and unsupervised pre-training for downstream tasks.

II. BACKGROUNDS

A. Entropy Estimators

For a random variable $x \in X$ with probability density function $p(x)$, Rényi's α -entropy [21] generalizes the definition of Shannon by introducing a hyperparameter α :

$$H_{x \in X}^\alpha(x) = \frac{1}{1-\alpha} \log_2 \left(\int_{x \in X} p^\alpha(x) dx \right), \quad (1)$$

when $\alpha \rightarrow 1$, we get back to Shannon's definition $-\int_{x \in X} p(x) \log_2 p(x) dx$.

Rényi entropy has been widely studied in statistics [22] and gained immense popularity in a wide range of applications in exploration RL [7, 9]. Its nice property is that it can be easily estimated with the matrix-based entropy functional [18]. Specifically, given N observations $\{\mathbf{s}_i\}_{i=1}^N$, its Gram or kernel matrix $K \in \mathbb{R}^{N \times N}$ can be obtained by $K(i, j) = \kappa(\mathbf{s}_i, \mathbf{s}_j)$, with κ denotes a kernel function which usually takes the form of Gaussian with width σ (i.e., $\kappa_\sigma(\mathbf{s}_i, \mathbf{s}_j) = \exp\left(-\frac{\|\mathbf{s}_i - \mathbf{s}_j\|_2^2}{2\sigma}\right)$), the state entropy can be evaluated as:

$$H_\alpha(\mathbf{s}) = \frac{1}{1-\alpha} \log_2[\text{tr}(A^\alpha)] = \frac{1}{1-\alpha} \log_2\left[\sum_{i=1}^N \lambda_i(A)^\alpha\right], \quad (2)$$

where "tr" is the matrix trace, $A = K / \text{tr}(K)$, $\lambda_i(A)$ denotes the i -th eigenvalue of A .

In this paper, we consider two other popular estimators including kernel density estimator (KDE) and k NN. KDE of the state set $\{\mathbf{s}_i\}_{i=1}^N$ is given by [23]:

$$H_{\text{KDE}}(\mathbf{s}) = -\frac{1}{N} \sum_{i=1}^N \log \left[\frac{1}{N} \sum_{j=1}^N \kappa(\mathbf{s}_i, \mathbf{s}_j) \right]. \quad (3)$$

Let $\mathbf{s}_i^{k\text{NN}}$ be the k NNs of \mathbf{s}_i , the k NN entropy estimator $H_{k\text{NN}}(\mathbf{s})$ is given by [13]:

$$H_{k\text{NN}}(\mathbf{s}) = \frac{1}{N} \sum_{i=1}^N \log \frac{N \cdot \|\mathbf{s}_i - \mathbf{s}_i^{k\text{NN}}\|_2^d \cdot \pi^{d/2}}{k \cdot \Gamma(d/2 + 1)} + C_k \quad (4)$$

in which $C_k = \log k - \Psi(k)$ is a bias correction constant, in which Ψ is the digamma function; Γ is the gamma function; d is the dimensionality of \mathbf{s} .

B. Reinforcement learning for exploration with maximum state entropy

The standard RL problem can be defined as policy search in an infinite-horizon Markov decision process (MDP) defined by a 5-tuple $(\mathcal{S}, \mathcal{A}, p, r, \gamma)$, where \mathcal{S} is the set of all possible states, \mathcal{A} is the set of actions, $p(\mathbf{s}_{t+1}|\mathbf{s}_t, \mathbf{a}_t) : \mathcal{S} \times \mathcal{A} \rightarrow \mathcal{S}$ is the transition probability density function. $\gamma \in [0, 1)$ is a discount factor. The episode $\tau = \{\mathbf{s}_1, \mathbf{s}_2, \dots\}$ constitutes state samples induced by a policy $\pi(\mathbf{a}_t|\mathbf{s}_t) : \mathcal{S} \rightarrow \mathcal{A}$. Meanwhile a stationary reward function $r(\mathbf{s}_t, \mathbf{a}_t) : \mathcal{S} \times \mathcal{A} \rightarrow \mathbb{R}$ is given, and the objective can be written as a maximization of the infinite-horizon discounted rewards:

$$J(\pi) = \mathbb{E}_{\tau \sim \pi} \left(\sum_{t=0}^{\infty} \gamma^t [r(\mathbf{s}_t, \mathbf{a}_t)] \right). \quad (5)$$

In scenarios where extrinsic/environmental rewards are unavailable, Early works by [8, 24] proposed to explore the environment by maximizing state entropy. More formally, the goal is to find an optimal policy π^* :

$$\arg \max_{\pi} H(p_{\pi}(s)) = \arg \max_{\pi} \left[- \int_{s \in \mathcal{S}} (p_{\pi}(s) \log(p_{\pi}(s))) \right] \quad (6)$$

where p_{π} denotes state distribution induced by π . Hazan et al [8] offer a provably efficient algorithm which internally splits state entropy in entropy gradients defined using probability density function of state. Multiple approaches have been proposed to enhance the method including Rényi variant [9], and efforts to reduce sample complexity [12]. Subsequently, Mutti et al. [5] consider a finite-horizon setting and introduce importance-weighted kNN entropy estimation for p_{π} . This method computes the implicit gradient of the state entropy estimate and maximizes it, resembling the framework of TRPO [25].

Building on previous works, Active Pre-Training (APT) [4] first adopts nearest neighbors as the intrinsic rewards r^i , which are directly proportional to the classic Kozachenko-Leonenko kNN entropy estimation in a non-parametric and model-free manner. The goal is simply to develop a reward function $r^i(\mathbf{s}_t, \mathbf{a}_t)$ as a substitute for r in Eq. (5). More formally:

$$r^i(\mathbf{s}) := \log(\|\mathbf{s} - \mathbf{s}^{k\text{NN}}\|_2 + 1), \quad (7)$$

where $\mathbf{s}^{k\text{NN}}$ denotes the neighbors of \mathbf{s} , and $\|\mathbf{s} - \mathbf{s}^{k\text{NN}}\|_2$ represents the norm of all k nearest neighbor distances to the state \mathbf{s} . It is important to note that most intrinsic rewards are **non-stationary**, which contradicts the standard MDP framework. Nonetheless, they achieve state-of-the-art performance when utilized to train deep reinforcement learning (DRL) agents in non-tabular environments, where $r^i(\mathbf{s}_t, \mathbf{a}_t)$ does not change rapidly.

Among all methods using this intrinsic reward function, ATP [4] first computes kNN distances in a representation space obtained through contrastive learning. Subsequently, [11] propose training an encoder simultaneously during exploration to obtain a prototypical representation space for the kNN computation in Eq. (7). RE3 [6] asserts that random encoders are sufficient in many cases, rather than requiring contrastive

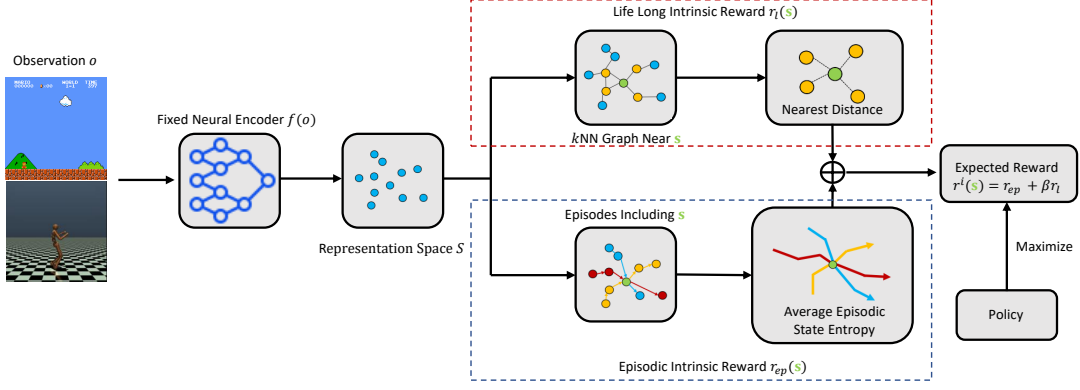


Fig. 1: Overview of our approach. The life long intrinsic reward of a state s (the **green** node) is computed as the distance to its k nearest neighbors, measured in representations space obtained from a fixed neural encoder. The episodic intrinsic reward is calculated as the average state entropy of these episodes including the state. The lifelong reward is then combined with episodic reward. A separate DRL is introduced for a policy that maximizes expected reward.

learning or a prototypical representation. Recently, RISE [7] extends it to Rényi entropy. Despite their flexibility and satisfactory performance in non-tabular environments, these methods lack episodic exploration, leading to the previously mentioned issue of vanishing lifelong rewards.

C. Parametric Methods for Exploration

In contrast to MaxEnt-based methods, parametric intrinsic rewards [16, 17, 26, 27] usually utilize an internal model to predict the next state and use the prediction error as the intrinsic motivation. These methods encourage agents to explore novel states in a lifelong manner by assigning greater rewards to states that are less frequently visited by estimating predictive forward models and use the prediction error as the intrinsic motivation. These *curiosity*-driven approaches, have their roots traced back to the 70's when Pfaffelhuber introduced the concept of “observer’s information” [28] and Lenat [29] introduced the concept of “interestingness” in mathematics to promote the novel hypotheses and concepts [3]. Recently popular prediction error-based approaches fall under this category. The recent surge in their popularity is strongly linked to the advancements in deep neural networks (DNNs). For instance, ICM [26] and RND [27], utilize a CNN as the internal model to predict the next image, while GIRIL implements variational autoencoder (VAE) to model the transitions in environments. After that, some approaches find the novelty vanishing problem and try to solve it by introducing episodic mechanism [16, 17]. However, the internal model introduces an auxiliary predictive task that brings additional complexities such as more hyper-parameters and increased running time.

III. INTRINSIC REWARD WITH ELEMENT

We focus on a fully unsupervised scenario in the absence of any extrinsic reward. The ELEMENT reward consists of two terms represented in blue and red respectively in Fig. 1: (1) episodic reward r_{ep} rapidly encourages visiting different states within the same episode, i.e., maximizing episodic state

entropy, (2) lifelong reward r_l slowly discourages visits to past states, visited many times in the history, i.e., maximizing lifelong state entropy. Both modules share the same fixed encoder $f(o)$, mapping the current observation o to a vectorized representation that we refer to as state s . More formally, the objectives of these two modules can be written as $\max H_{s \in \tau}(s)$, where $\tau = \{s_t\}_{t=1}^{T_\tau}$ represents an episode that constitutes T_τ cascade state samples, and $\max H_{s \in D}(s)$, with $D = \{s_i\}_{i=1}^N$ being a global memory that archives all previous visited states, respectively. The intrinsic reward with ELEMENT is constructed by adding both rewards:

$$r^i(s) = r_{ep}(s) + \beta r_l(s), \quad (8)$$

where β is a positive hyper-parameter weighting the relevance of the latter. An illustrative example demonstrating the impact of episodic and lifelong exploration is shown Fig. 2. The Mujoco ant agent is capable of navigating freely in all directions within a 3D space, starting from the center. When trained solely with $r_{ep}(s)$, the agent tends to move in a single direction, maximizing the number of distinct states in a single episode. Conversely, when trained only with $r_l(s)$ alone, the agent is discouraged from exploring previously visited directions, and thus hard to fully explore a direction. Our approach integrates both motivations: $r_{ep}(s)$ constrains the agent to generate episodes consisting exclusively of distinct states, while $r_l(s)$ persistently encourages the agent to explore unvisited states by fostering the creation of such episodes. As a result, during each episode, the agent consistently moves radially in one direction. If we continue the training process, the ELEMENT agent explores the world more radially, akin to “fireworks”. Ablation studies examining the effects of varying β can be found in Section IV-F.

A. Fixed neural encoder $f : \mathcal{O} \rightarrow \mathcal{S}$.

The parametric encoder maps the current observation to a d -dimensional state s . Consider a changing encoder that leads to very different representation (state) for the same observation, an agent could visit a large number of different ‘states’ without

taking any actions. To avoid such meaningless exploration, the encoder must be pre-trained and fixed before the exploration agent starts to learn. In this paper, we adopt two encoders for Mujoco and Mario environments, respectively. For Mujoco, we implement a fixed randomly initialized neural encoder which has been empirically validated for state entropy estimation [6]. For Mario, we pre-train an encoder using Spatiotemporal Deep Infomax [30], a contrastive state representation learning method that maximizes the mutual information across both the spatial and temporal axes. This could become a limitation in environments where it is difficult to collect sufficient data for representation learning, as detailed in Section V.

B. Episodic intrinsic reward.

The major challenge for episodic entropy maximization is that intrinsic rewards based on episodes instead of current state-action pairs subtly changes the underlying MDP into an episodic POMDP problem: an agent receives a single feedback $R_{ep}(\tau) = H_{s \in \tau}(\mathbf{s})$ only at the conclusion of each episode, as discussed above. To solve this problem, we assume the existence of an underlying standard MDP reward function $r_{ep}(\mathbf{s}_t, \mathbf{a}_t)$ that approximates the episodic reward $R_{ep}(\tau)$ in a sum-form decomposition $R_{ep}(\tau) \approx \sum_{t=1}^{T_\tau} r_{ep}(\mathbf{s}_t)$, which is a common trick for trajectory-wise feedback problems [31, 32, 33]. More formally, the episodic objective is decomposed to learn an optimal policy by maximizing:

$$\begin{aligned} J_{ep}(\pi) &= \mathbb{E}_{\tau \sim \pi} [R_{ep}(\tau)], \\ &= \mathbb{E}_{\tau \sim \pi} [H_{s \in \tau}(\mathbf{s})], \\ &\approx \mathbb{E}_{\tau \sim \pi} \left[\sum_{t=0}^{T_\tau-1} r_{ep}(\mathbf{s}_t, \mathbf{a}_t) \right]. \end{aligned} \quad (9)$$

Given such a Markovian proxy reward function $r_{ep}(\mathbf{s}_t, \mathbf{a}_t)$, the agent can be trained using any standard RL algorithms. A popular approach to model r_{ep} involves parameterization by effectively minimizing the objective function [32, 33]:

$$\mathcal{L}(r_{ep}, \theta) = \mathbb{E}_{\tau \in D} \left[\left(H_{s \in \tau}(\mathbf{s}) - \left[\sum_{t=0}^{T_\tau-1} r_{ep}(\mathbf{s}_t, \mathbf{a}_t, \theta) \right] \right)^2 \right], \quad (10)$$

where θ denotes the parameters of the learned reward model. However, parametric modeling introduces additional uncertainties due to hyper-parameters, fine-tuning, etc. Instead, inspired by episode-space smoothing [31], we define our non-parametric episodic intrinsic reward as:

$$r_{ep}(\mathbf{s}) := \mathbb{E}_{\tau \in D} [H_{s_i \in \tau}(\mathbf{s}_i) \cdot \mathbb{I}(\mathbf{s} \in \tau)] \quad (11)$$

where $H_{s_i \in \tau}(\mathbf{s}_i)$ denotes the estimated state entropy value using all states within the episode τ . $\mathbb{I}(\mathbf{s} \in \tau)$ is an indicator function representing whether the trajectory τ includes (\mathbf{s}) . This reward function allows for flexibility in selecting any suitable estimator. In this paper, we consider three different estimators defined in Section II and select one based on their experimental performance. The intuitive aim of this reward function is to gauge the ‘‘average entropy’’ of a state \mathbf{s} based on the episodes accumulated during the training process. States that consistently appear in high-entropy episodes are assigned

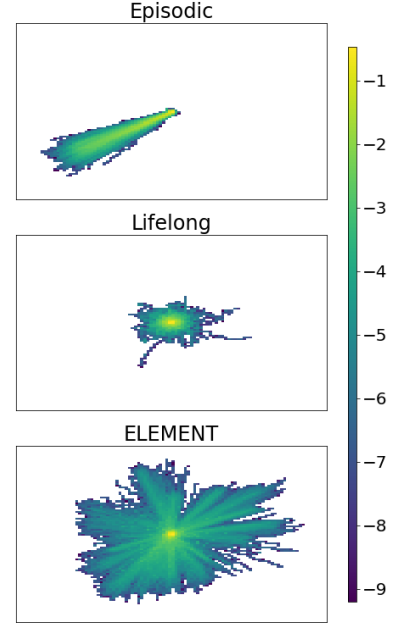


Fig. 2: Episodic entropy maximization encourages movement in a single direction to capture more distinct states per episode. Deviating from this direction will result in smaller distances to the previously visited states within the same episode. Lifelong motivation discourages revisiting episodes, hindering a continual exploration towards one direction. ELEMENTs shares merits of both, promoting comprehensive exploration without confinement to one direction.

larger rewards. Theoretically, implementing Eq. (11) provides an optimal solution for an upper bound to the loss function described in Eq. (10):

Proposition 1. Assume all episodes have the same length T_τ , we define an upper bound of Eq. (10) given by the Monte-Carlo estimation [32]:

$$\tilde{\mathcal{L}}(r_{ep}) = \mathcal{L}(r_{ep}) + \mathbb{E}_{\tau \in D} [T_\tau^2 \cdot V_{s \in \tau}(r_{ep}(\mathbf{s}))] \quad (12)$$

where $V_{s \in \tau}(r_{ep}(\mathbf{s})) \geq 0$ denotes the expected variance of rewards within the episodes. The optimal solution r_{ep}^* to minimize $\tilde{\mathcal{L}}(r_{ep})$ is given by:

$$r_{ep}^*(\mathbf{s}) = \mathbb{E}_{\tau \in D} \left[\frac{H_{s_i \in \tau}(\mathbf{s}_i)}{T_\tau} \cdot \mathbb{I}(\mathbf{s} \in \tau) \right] \quad (13)$$

A minor difference between Eq. (11) and Eq. (13) is a scale T_τ which is a constant. Proofs and extended discussion for different T_τ are provided in Appendix A.

C. Lifelong intrinsic reward.

The trick of the sum decomposition for episodic state entropy, i.e., $H_{s \in \tau}(\mathbf{s}) \approx \sum_{t=1}^{T_\tau} r_{ep}(\mathbf{s}_t)$ in Eq. (9), and its solution in Eq. (11) are not suitable for lifelong scenario, because no estimator can effectively estimate the entropy across all visited states, which could number more than dozens of millions. To make the above mentioned estimators amenable to lifelong scenario, we instead pursue an intrinsic reward propositional to the entropy estimation: $H_{s \in D}(\mathbf{s}) \propto \sum_{i=1}^N r_l(\mathbf{s}_i)$. More formally, we provide Proposition 2 which identifies the relationships between entropy estimators and k NN distances.

Proposition 2. Given N states $\{\mathbf{s}_i\}_{i=1}^N$ and a Gaussian kernel κ with kernel width σ , let \mathbf{s}_i^{kNN} be the k -nearest neighbors (kNN) of \mathbf{s}_i , we consider $\sum_{j=1}^N \kappa(\mathbf{s}_i, \mathbf{s}_j) \approx \sum_{j \in kNN} \kappa(\mathbf{s}_i, \mathbf{s}_j)$ if $|\sum_{j=1}^N \kappa(\mathbf{s}_i, \mathbf{s}_j) - \sum_{j \in kNN} \kappa(\mathbf{s}_i, \mathbf{s}_j)| \leq \epsilon$, where ϵ is the approximation tolerance¹. The kernel density estimator (KDE), kNN estimator and 2nd-order matrix-based Rényi's entropy estimator (i.e., $\alpha = 2$) are proportional to a function in the form of kNN distances:

$$H_{KDE}(\mathbf{s}) \propto \frac{1}{N} \sum_{i=1}^N [-\log[\sum_{j \in kNN} \kappa(\mathbf{s}_i, \mathbf{s}_j)]]$$

$$\text{if } \forall \mathbf{s}_i, \max_{\mathbf{s}_j \in \mathbf{s}_i^{kNN}} \|\mathbf{s}_i - \mathbf{s}_j\| \geq \left[2\sigma \log \frac{N-k}{\epsilon}\right]^{\frac{1}{2}}, \quad (14a)$$

$$H_{kNN}(\mathbf{s}) \propto \frac{1}{N} \sum_{i=1}^N \log \sum_{j \in kNN} \|\mathbf{s}_i - \mathbf{s}_j\|_2$$

$$= \frac{1}{N} \sum_{i=1}^N \log \|\mathbf{s}_i - \mathbf{s}_i^{kNN}\|_2. \quad (14b)$$

$$H_2(\mathbf{s}) \propto \log \sum_{i=1}^N [-\sum_{j \in kNN} \kappa(\mathbf{s}_i, \mathbf{s}_j)],$$

$$\text{if } \forall \mathbf{s}_i, \max_{\mathbf{s}_j \in \mathbf{s}_i^{kNN}} \|\mathbf{s}_i - \mathbf{s}_j\| \geq \left[2\sigma \log \frac{N-k}{\epsilon}\right]^{\frac{1}{2}}. \quad (14c)$$

Previous kNN -based approaches [4, 6, 7] essentially implement the kNN estimator, i.e., the second relation in Eq. (14). However, the computational complexity associated with kNN remains a challenge due to the large number of visited states. These methods often resort to using a first-in-first-out queue or sample a limited number of states to compute nearest distances. This compromise impedes their ability to meet the real lifelong goal due to rapid “forgetting” or downsampling of states.

To address this challenge, we utilize a kNN graph to efficiently organize all visited states, reducing the computational load and enhancing performance. A kNN graph is a directed graph $\mathcal{G} = (D, \mathcal{E})$, where \mathcal{E} is the set of links. Node \mathbf{s}_i is connected to node \mathbf{s}_j if \mathbf{s}_j is one of the kNN s of \mathbf{s}_i . Let $\mathbf{s}^{kNN} = \text{GNNS}(\mathcal{G}, \mathbf{s})$ be the graph nearest neighbor search (GNNS) algorithm which returns kNN of \mathbf{s} , our lifelong intrinsic reward proportional to kNN entropy estimator can be defined as:

$$r_l(\mathbf{s}) := \log(\|\mathbf{s} - \text{GNNS}(\mathcal{G}, \mathbf{s})\|_2 + 1), \quad (15)$$

We have chosen the kNN entropy estimator for its widespread validation in exploration tasks [6, 7, 17] and because it has fewer constraints compared to other estimators, as outlined in Proposition 2.

In practice, we found Fast Approximate GNN Search [19] and Fast Online kNN Graph Building [20] worked well. In Fast Approximate GNN Search (see the left panel of Fig. 3), starting from randomly chosen nodes from the kNN graph, the

algorithm simply replaces the current nodes by the neighbor that is closest to the query. Fast Online kNN Graph Building is then used to update the graph \mathcal{G} . As shown in the right panel of Fig. 3, it uses its neighbors as starting points to search existing nodes for which the new point is now a nearest neighbor, up to a fixed depth. Details can be found in Algorithm 1 and 2.

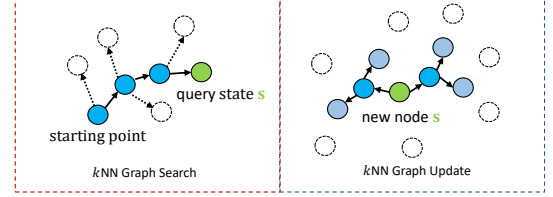


Fig. 3: The kNN graph search and online update algorithms on simple nearest neighbor graphs. In searching phase, the algorithm search by moving to the neighbor that is closest to the query. After that, neighbors obtained by the search phase are used as starting points to update existing nodes for which the new point is now a nearest neighbor.

Algorithm 1 Fast Approximate GNN Search algorithm

Require: a kNN graph, query \mathbf{s} , the number of greedy search steps $R1$, the number of random restarts $R2$. Let $ND(X)$ returns k nearest neighbors of X according to the graph. $E = \{\}$

- 1: **for** all $R2$ in parallel: **do**
- 2: Sample a random node $X0$ from the graph.
- 3: **for** $R1$ steps: **do**
- 4: $Y = ND(X0)$.
- 5: Find the node closest to query \mathbf{s} with Y , denoted as $X0'$.
- 6: $X0 = X0'$.
- 7: **end for**
- 8: Append $X0$ to E .
- 9: **end for**
- 10: **return** k closest nodes to query \mathbf{s} within E .

Algorithm 2 Fast kNN online update algorithm

Require: the current knn graph; new node \mathbf{s} ; k neighbors of the new node \mathbf{s} , denoted as a list A . Let $ND(X)$ returns k nearest neighbors (edges) of X according to the graph. Let $Dis(X, \mathbf{s})$ returns distances between X and \mathbf{s} .

- 1: **for** d in depth: **do**
- 2: **for** all nodes within A : **do**
- 3: $X = A.pop()$.
- 4: $Y = ND(X0)$.
- 5: Append nodes in Y to A .
- 6: **if** $Dis(X, \mathbf{s}) < Y.any()$: **then**
- 7: Replace the longest edge of X with $Dis(X, \mathbf{s})$.
- 8: **end if**
- 9: **end for**
- 10: **end for**
- 11: **return** The updated kNN graph

¹Note that, for any sample \mathbf{s}_m that is far away from \mathbf{s}_i , $\kappa_\sigma(\mathbf{s}_i, \mathbf{s}_m) = \exp\left(-\frac{\|\mathbf{s}_i - \mathbf{s}_m\|_2^2}{2\sigma}\right) \rightarrow 0$.

Algorithm 3 ELEMENT for Off-Policy RL.

```

1: Initialize policy, Set  $k$ ,  $k$ NN graph  $\mathcal{G}$ .
2: Set a batch size  $N$ , a graph update interval  $U$  and graph
  update step number  $T_u$ ,  $\beta$ .
3: Clear global replay buffer:  $D = \emptyset$ .
4: for every time step  $t$  do
5:   Clear local replay buffer  $D_\tau = \emptyset$ 
6:   for every step in an episode  $\tau$  do
7:      $\mathbf{a}_t \sim \pi(\mathbf{a}_t|\mathbf{s}_t)$ 
8:      $\mathbf{s}_{t+1} \sim P(\mathbf{s}_{t+1}|\mathbf{s}_t, \mathbf{a}_t)$ 
9:      $D_\tau \cup \{(\mathbf{s}_{t+1}, \mathbf{s}_t, \mathbf{a}_t)\}$ 
10:    if  $0 < (t \bmod U) < T_u$  and  $t|U \neq 0$  then
11:      Update  $\mathcal{G}$  with  $\mathbf{s}_{t+1}$ 
12:    end if
13:  end for
14:  Estimate  $r_{ep} = H_{\mathbf{s} \in D_\tau}(\mathbf{s})$ .
15:  for every sample  $(\mathbf{s}_{t+1}, \mathbf{s}_t, \mathbf{a}_t)$  in  $D_\tau$  do
16:     $D \cup \{(\mathbf{s}_{t+1}, \mathbf{s}_t, \mathbf{a}_t, r_{ep})\}$ 
17:  end for
18:  for every policy update steps do
19:     $\{\mathbf{s}_{t+1}^{(n)}, \mathbf{s}_t^{(n)}, \mathbf{a}_t^{(n)}, r_{ep}^{(n)}\}_{n \leq N} \sim D$ 
20:    Compute  $r_l$  using Eq. (15).
21:    Normalize  $r_{ep}$  and  $r_l$ 
22:     $r^i = r_{ep} + \beta r_l$ 
23:    Update policy
24:  end for
25: end for

```

Thanks to the fast k NN graph, the total computational complexity for calculating lifelong intrinsic rewards decrease from $\mathcal{O}(N^2)$ to $\mathcal{O}(Nk(R1R2 + k^{d-1}))$, where $R1, R2$ and d are fixed hyper-parameters related to number of searching steps.

Combining episodic and lifelong rewards, we provide the off-policy RL pipeline of our method in Algorithm 3. On-policy RL algorithms can be adapted with a minor modification: record the episodic state entropy values for each state and assign the average entropy values of $\mathbf{s}^{k\text{NN}}$ to r_{ep} . Recall that lifelong exploration *slowly* discourages revisits to visited states, and thus we introduce two hyper-parameters: graph update interval U and update step number T_u . These parameters dictate that the graph is updated every U training steps for T_u steps.

IV. EMPIRICAL ANALYSIS

The experimental section is organized as follow. In **Section IV-A**, we qualitatively illustrate how ELEMENT explores the environment. Afterwards, we quantitatively demonstrate that ELEMENT outperforms other SOTA intrinsic rewards, including RND [27], NGU [17], RE3 [6] and RISE [7], in maximizing episodic state entropy (**Section IV-B**) and number of visits in lifelong mode (**Section IV-C**). Importantly, the samples collected by ELEMENT can be effectively used for offline learning, as illustrated in **Section IV-D**. Besides, we show that ELEMENT is an effective unsupervised pre-training method for downstream tasks in **Section IV-E**. Additional

experiments including ablation study and visualizing reward distribution are provided in **Section IV-F and IV-G**, respectively. We implement the Soft Actor Critic (SAC) [34] for the Mujoco environments and Asynchronous Advantage Actor-Critic (A3C) [35] for Mario as the respective backbone algorithms. In the subsequent experiments, we set β to 0.5 after normalizing both r_{ep} and r_l to the range $[0, 1]$. Details of other experimental settings are available in **Appendix 1b**.

A. How Does ELEMENT Drive the Agent?

We employ Walker2D, Ant and Mario environments from the Mujoco and NES simulation suite to qualitatively visualize the exploration process during training. In Walker2D, the agent can only move forward or backward within a 2D spatial plane, whereas the Ant agent can navigate freely in all directions within a 3D space. Both agents are reset to starting points near $(0, 0)$ if they fail to meet the health conditions specified by the default setting [36]. The default number of steps for truncation in these environments is directly adopted as T_τ , without any fine-tuning.

To observe policies in the entire training process, we establish checkpoints every 500,000 steps and execute the trained policies π_c to collect 30,000 samples at these checkpoints, where π_c denotes the policy at c -th checkpoint. We also synchronize the graph update interval with these checkpoints, setting $U = 500,000$. The trajectories executed by π_c are depicted using different colors in Fig. 4. For visualization, we track and record the x - z and x - y coordinates, respectively.

As shown by the trajectories generated by π_1 , the agent learns to move backward in Walker2D and upward in Ant, driven purely by episodic entropy maximization, as the k NN graph remains empty before the first checkpoint. This episodic strategy leads to sequences characterized by high episodic state entropy but lacks variance across different episodes. This finding empirically validate that ELEMENT achieves the episode goal which encourages an agent to revisit familiar states over several recent episodes, but not within the same episode. Subsequently, as the k NN graph begins to update periodically, it prompts agents to explore novel states while still adhering to policies that maximize episodic state entropy. Consequently, this exploration strategy uncovers a variety of episodes with diverse states. These episodes include various motion skills including moving in different directions, walking, running, and jumping with different legs. **Videos** detailing these behaviors are available in the supplementary files.

B. Can ELEMENT Maximize Episodic State Entropy?

Recall that ELEMENT assumes the existence of an additive form of the episodic state entropy, i.e., $\mathbb{E}_\tau[H_{\mathbf{s} \in \tau}(\mathbf{s})] \approx \mathbb{E}_\tau\left[\sum_{t=0}^{T_\tau-1} r_{ep}(\mathbf{s}_t)\right]$. In this section, we first empirically validate this underlying assumption. We train a SAC agent in the Ant environment using default task-driven rewards and record all historical states during the training process. Subsequently, we train a deep neural network (DNN) $r_\theta(\mathbf{s})$ to model $r_{ep}(\mathbf{s})$ using these approximately 2,000 historical trajectories by minimizing the objective function $\|H_{\mathbf{s} \in \tau}(\mathbf{s}) - \sum_{t=0}^{T_\tau-1} r_\theta(\mathbf{s}_t)\|_2$ over all trajectories in the dataset. Fig. 5 (a) presents the

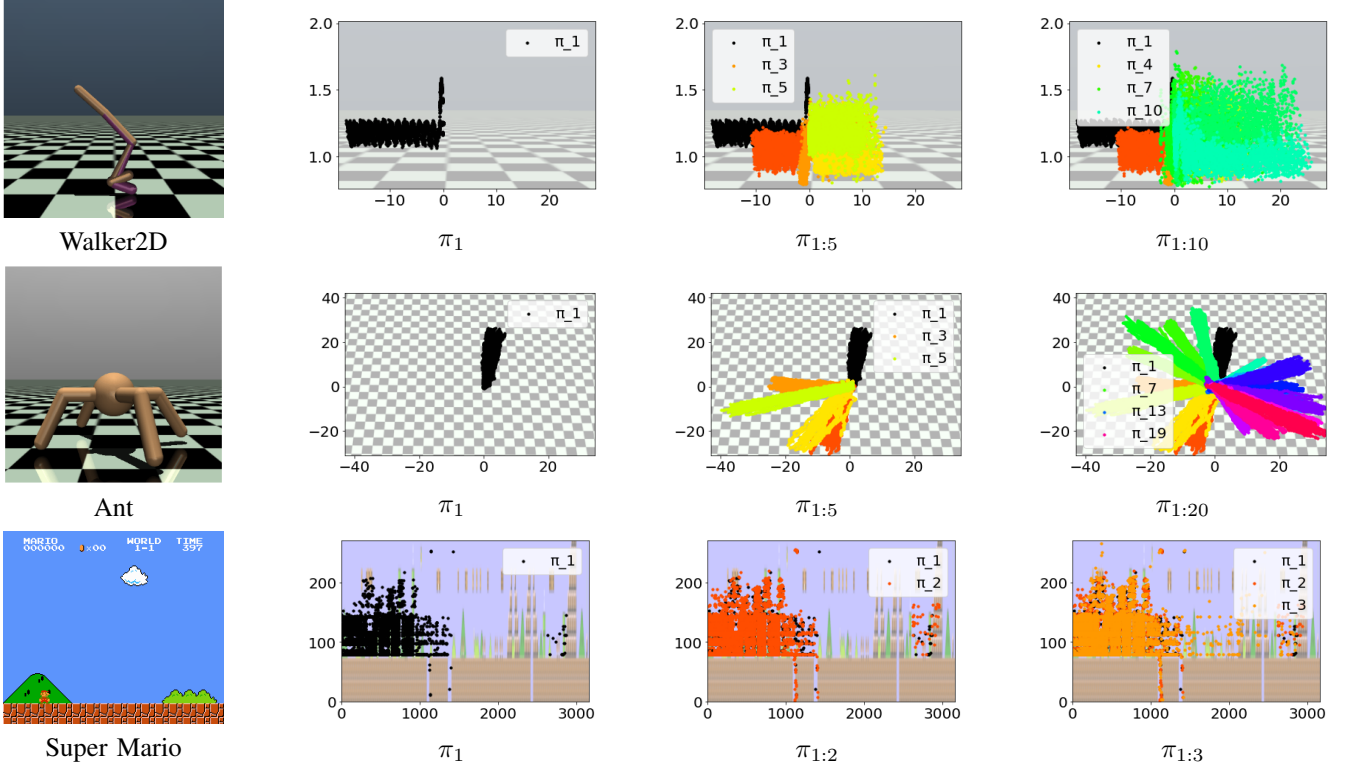


Fig. 4: Trajectories obtained by executing policies at different checkpoints (depicted by different colors) on Walker2D, Ant and Mario. At the first checkpoint, the agent quickly converges to a policy which produces similar episodes with many different states. When the learning process continues and the k NN graph gradually updates, agents slowly try to stay away from visited episodes but still make states within an episode different.

learning curve, where the loss is minimized, and the predicted episodic entropy (b) closely aligns with the ground truth. This demonstrates that it is reasonable to assume the existence of such a reward function.

Furthermore, we compare our approach with baselines in Mujoco and Mario environments, using Shannon entropy within each trajectory as our evaluation metric. This comparison aims to empirically demonstrate our method’s superiority in maximizing episodic state entropy, i.e., $\max H_{s \in \tau}(s)$. Therefore, we solely implement the proposed episodic rewards, setting $\beta = 0$ in Eq. (8). The episodic state entropy for evaluation in this section is estimated with the matrix-based entropy functional in Eq. (2) with $\alpha = 1.001$. We train the ELEMENT framework using only episodic rewards, r_{ep} . The learning curves, with the y -axis representing Shannon state entropy, are illustrated in Fig. 6. Experiments are repeated for 10 times, and we report average scores with variance. Overall, our method surpasses baselines in both exploration range and sample efficiency.

C. Can ELEMENT Explore New States Efficiently?

In the following, we compare our approach with baselines using unique visited state in the entire training process as our evaluation metric. Given the continuous high-dimensional state spaces, counting visited states becomes practically challenging. To manage this, we discretize only x - y or x - z coordinates into 100×100 histograms. Subsequently, we count

unique visited states in the entire training process. We train the ELEMENT framework using both episodic and lifelong rewards. The learning curves, with the y -axis representing unique visited spatial coordinates, are illustrated in Fig. 7. Experiments are repeated for 5 times, and we report average scores with variance. Overall, our method surpasses the baseline methods in terms of both exploration range and sample efficiency.

D. Can the Samples Collected by ELEMENT Agents be Used for Offline learning?

The results in Section IV-C indicate that ELEMENT could have a significantly potential impact on unsupervised offline RL[37], which first collect state samples during a sampling phase and then learn from these samples during the training phase. It is widely accepted that “more visited states will result in improved performance in offline learning [38].

In this section, we conduct offline reinforcement learning (RL) on samples induced by ELEMENT and baseline agents. During the exploration phase, we interact with the environment using the trained exploration policies recorded throughout the unsupervised training process, i.e., $\{\pi_1, \pi_2, \dots\}$, as illustrated in Fig. 4, to collect samples $\{s_{t+1}, a_t, s_t, r(s_t, a_t)\}$ over 1,000,000 steps. Here, $r(s_t, a_t)$ represents the task-driven extrinsic reward. In the planning phase, we train an offline RL algorithm using the collected dataset, thus eliminating the need for further interaction with the environment. For our

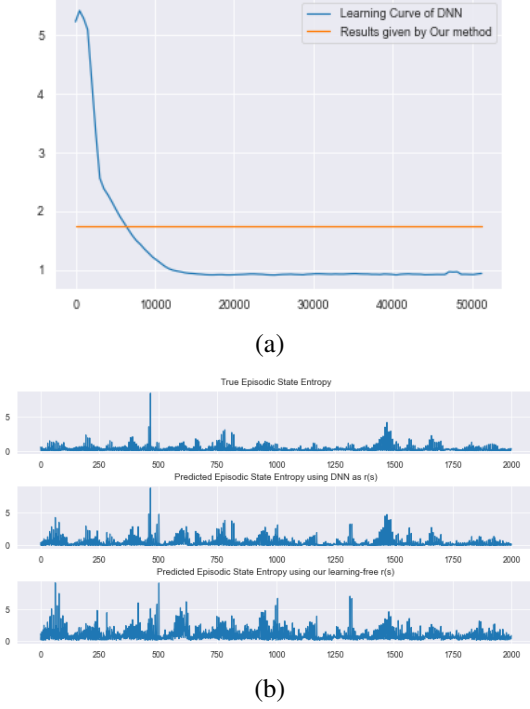


Fig. 5: (a) The learning curve given by parametric modeling of the episodic reward $r_{ep}(s)$ using a DNN. (b) Predicted episodic state entropy using $r_{ep}(s)$ in ELEMENT.

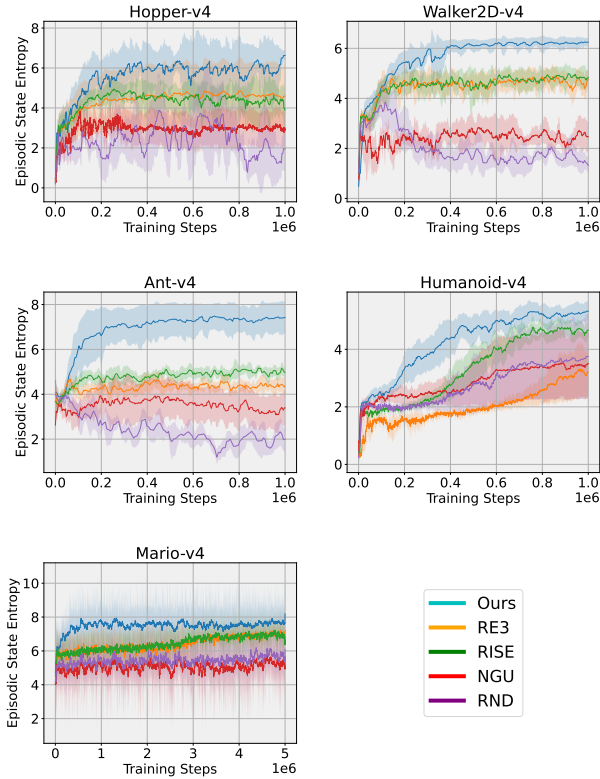


Fig. 6: Performance of episodic state entropy maximization. The y -axis represents Shannon state entropy within an episode, which is estimated using matrix-based entropy functional [18] with $\alpha = 1.001$.

experiments, we employ the Conservative Q-Learning (CQL)

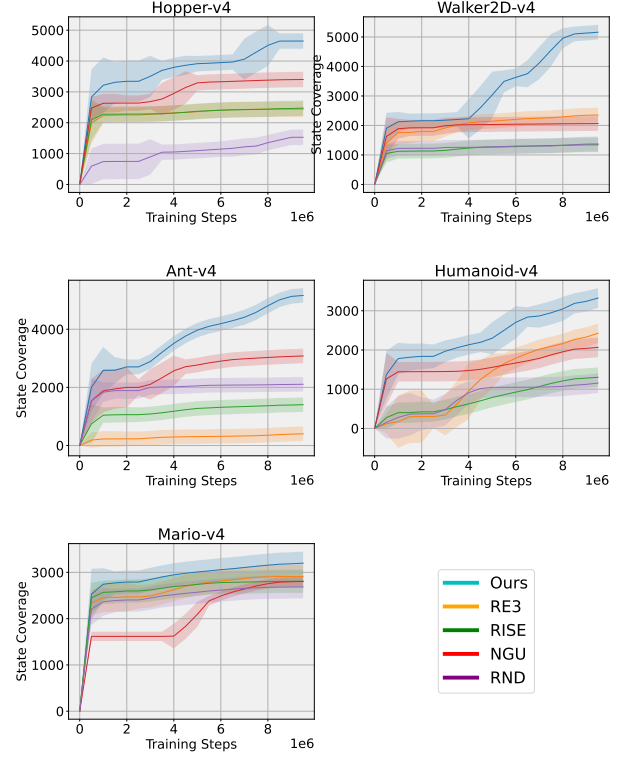


Fig. 7: Performance of lifelong state entropy maximization. Evaluated by state coverage, i.e., total unique visited states in the training process.

algorithm [39] as the offline RL method.

Table I summarizes the results across five environments. We normalize the score of online SAC to 1 and the score of a random policy to 0. Overall, our method outperforms the baseline methods in terms of task-driven scores. It is important to note that the results are highly dependent on the choice of offline RL algorithm. For example, when using behavioral cloning (BC) [40], the score of the random policy on Humanoid can be as low as approximately 0.

For the sake of simplicity and popularity, we have chosen to use the widely adopted CQL method for our preliminary experiments, as the specific choice of offline RL algorithm is beyond the scope of this paper.

E. Can ELEMENT agents Conduct Task-Agnostic Exploration for Downstream Tasks?

In this section, we demonstrate the benefits to an agent from an exploration policy learned by ELEMENT. After unsupervised pre-training with ELEMENT and other baselines, the learned policies are assessed on downstream tasks. We establish 10 checkpoints for each method during their learning process. The policy that demonstrates the highest task-driven rewards at these checkpoints is selected for transfer to downstream tasks. The learning curves for episodic extrinsic returns are illustrated in Fig. 8. These experiments were conducted 5 times to ensure reliability, with average scores and variances reported. For clarity, we applied a smoothing window to the curves. ELEMENT pre-training consistently enhanced performance across tasks, contrasting with the notably slower

Environments	ELEMENT (Ours)	RE3	RISE	NGU	RND
Hopper	0.516 ± 0.075	0.469 ± 0.051	0.534 ± 0.076	0.391 ± 0.040	0.271 ± 0.073
Walker2D	0.212 ± 0.043	0.111 ± 0.024	0.120 ± 0.059	0.201 ± 0.082	0.106 ± 0.036
Ant	0.142 ± 0.072	0.137 ± 0.347	0.126 ± 0.018	0.107 ± 0.026	0.110 ± 0.023
Humanoid	0.373 ± 0.048	0.071 ± 0.036	0.100 ± 0.081	0.131 ± 0.054	0.256 ± 0.031
Mario	0.481 ± 0.012	0.402 ± 0.208	0.352 ± 0.159	0.423 ± 0.026	0.359 ± 0.023

TABLE I: Comparing the samples collected by NGU, RND, RISE, RE3, and ELEMENT exploration methods for offline learning, normalized with respect to the random policies and the online Soft Actor-Critic (SAC) method. The best performance is in bold.

learning from scratch. In the Hopper, Walker2D, Humanoid and Mario, ELEMENT enabled zero-shot policy optimization, as the unsupervised exploration phase had already uncovered optimal behaviors. Ant is an exception where all exploration agents remain stuck in sub-optimal motion modes after pre-training, resulting in their performance being outpaced by SAC agents trained from scratch. However, ELEMENT shows promising initial performance and converges faster than other exploration baselines.

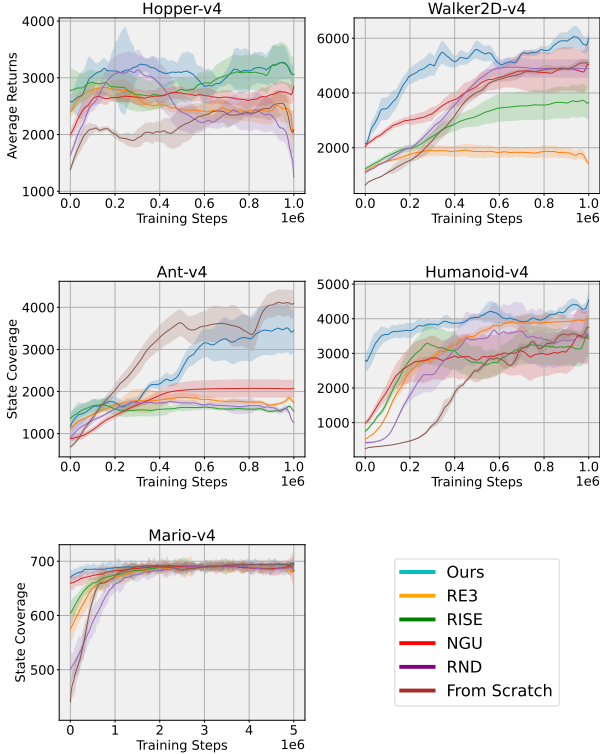


Fig. 8: Performance of agents in downstream tasks after unsupervised pre-training the agent.

F. Ablation Study for β

In this section, we extend the experiments presented in Fig. 2 and analyze the impact of β in detail. The Ant agent in Mujoco can navigate freely in all directions within a three-dimensional space. Both agents are reset to randomly initialized starting points near (0, 0) if they fail to meet the health conditions specified by the default gym-Mujoco package. The default number of steps for truncation is set to 1000, which is directly adopted as T_τ without any fine-tuning. Both r_{ep} and r_l are normalized to the range [0, 1] using min-max normalization. The Soft Actor-Critic (SAC) algorithm

serves as the backbone for this analysis. For visualization purposes, we record the x-y coordinates and color them based on logarithmic probability. As illustrated in Fig. 9, the length

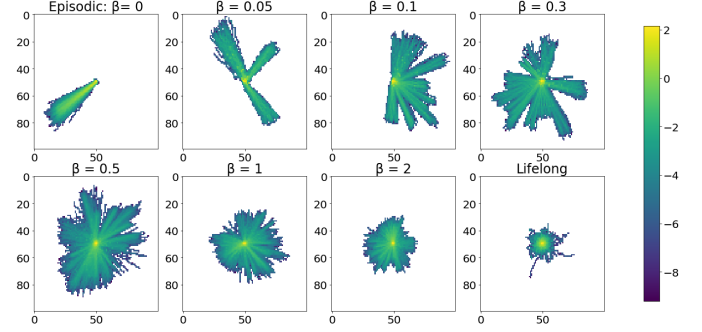


Fig. 9: Trajectories obtained during the training process using different β . Colored by logarithmic probability.

of exploration episodes (radius) decreases with the increasing impact of lifelong exploration. This observation validates that lifelong exploration constrains “deep” exploration in a single direction. Conversely, when episodic exploration has a greater contribution (i.e., small β), agents are able to explore regions that are farther away from the starting points. Additionally, we note that the number of angles increases with the growing influence of lifelong exploration. Thus, lifelong exploration encourages the agent to investigate a greater variety of directions, whereas episodic exploration tends to limit this. In summary, ELEMENT with an appropriate β , such as 0.5, effectively balances episodic and lifelong exploration, thereby promoting exploration in both radius and angular dimensions.

G. How Does ELEMENT Assign Intrinsic Rewards?

We utilize a 20×20 discrete maze² for visualizing intrinsic rewards at each state during training. Agents begin to explore from the top-left corner and navigate for 700 steps per trial, returning to the top-left corner afterwards. We compare episodic and lifelong rewards distributions by training agent with r_{ep} or r_l only. Since the maze is simple and the number of states is finite, we simply implement brute k NN instead of a graph. We employ classic Q-learning as the oracle and update the Q-tables over a course of 300×700 steps.

Fig. 10 displays snapshots of the reward distributions at intervals of 5×700 , 50×700 , and 300×700 steps. Lifelong rewards initially motivate agents to explore new areas during the early training phase. Notably, by the 50-th episode, they assign large rewards to states deeper in the maze. As the training advances and agents more frequently reach the deeper

²https://github.com/giorgionicoletti/deep_Q_learning_maze

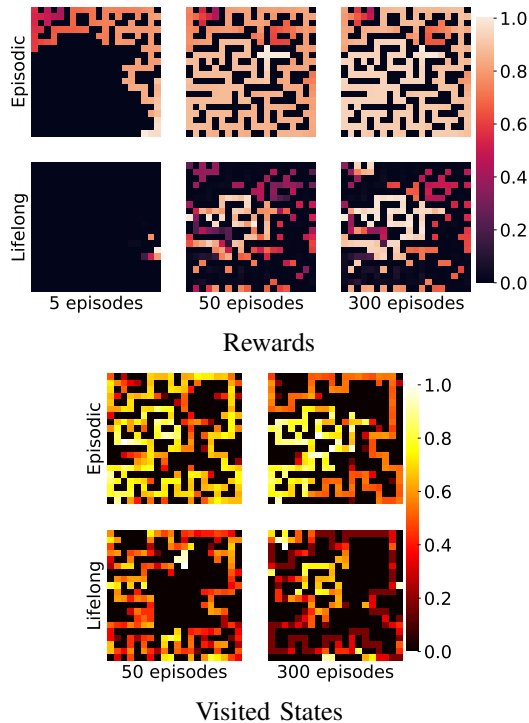


Fig. 10: The left panel displays the rewards assigned to each state during the training process by episodic and lifelong rewards, while the right panel depicts the corresponding trajectories generated based on agents optimized using these rewards.

states, there is a gradual increase in rewards for states near the starting point (shallow states), while the rewards for paths leading to these deeper states correspondingly decrease. As a result, by the 300-th episode, agents often find themselves trapped in dead ends near the starting point.

In contrast, episodic agents distribute state entropy rewards smoothly and effectively across the maze, reaching even the deepest parts. Intuitively, previous reward functions overlook a crucial aspect: some of these frequently visited states may serve as essential gateways to the lesser-explored areas that require investigation. Instead, episodic stance is that reward distribution should be designed to smoothly navigate agents towards exploring a broader array of states within each episode.

V. LIMITATION AND FUTURE WORKS

a) Fixed Encoders.: The primary limitation of ELEMENT is its reliance on a fixed encoder, avoiding that distinct representations correspond to the same observation. However, this introduces a chicken-and-egg dilemma in long-horizon environments: obtaining diverse observations for robust representation learning is challenging without effective exploration strategies, and conversely, it's difficult to develop proficient exploration RL without a solid foundation in representation learning. This issue is common across nearly all non-parametric exploration RL methods. Addressing this challenge is a key objective for our future research.

b) Trade-off influenced by episode length T_τ .: Given the proposition 1, the tightness of the upper bound is determined by the expected variance by the expected variance

$\mathbb{E}_{\tau \in D}[T_\tau^2 \cdot V_{s \in \tau}(r_{ep}(s))]$. Typically, longer episodes lead to higher variances in state rewards, resulting in a looser bound. Conversely, estimation accuracy generally improves as the number of samples increases, which is typical of longer episodes. Here, we identify a trade-off influenced by the episode length T_τ . Specifically, a longer episode leads to a reduced entropy estimation error, but at the cost of an increased Monte-Carlo estimation error.

VI. CONCLUSION

We develop ELEMENT, a novel intrinsically motivated RL exploration framework to foster state entropy maximization from both episodic and lifelong perspectives. The two objectives inside ELEMENT are complementary to each other and enable the usage of popular entropy estimators. Episodic entropy maximization ensures to search deeper by visiting diverse states in each episode, whereas lifelong entropy maximization enables to search wider by visiting different states across episodes. We test ELEMENT in robotic Mujoco and Mario environments. Qualitatively, we demonstrate how ELEMENT rewards guides agents to produce episodes with high state entropy permanently, and to slowly move away from visited states. Quantitatively, episodes generated by ELEMENT achieve the highest episodic state entropy and largest number of unique visited states, compared to SOTA approaches. Offline RL methods trained with data collected by ELEMENT also outperform those trained with data collected by baseline methods. Additionally, ELEMENT learns various motion skills unsupervisedly, and thus significantly outperforms baselines in task-agnostic exploration for downstream tasks.

Our ELEMENT has two limitations, which we leave for future work. First, we utilize a fixed encoder that is obtained through pre-training. In long-horizon environments, it may be challenging to collect sufficient data for effective pre-training. Second, the episodic module presents a trade-off in terms of episodic length where longer episodes lead to reduced entropy estimation errors, but at the cost of increased Monte-Carlo estimation errors.

APPENDIX

BASELINE DETAILS

Here is a brief introduction to our baselines.

The **Random Network Distillation (RND)** [27] is a parametric exploration method driven by curiosity. Utilizing prediction errors to measure novelty, this approach predicts the output of a fixed randomly initialized neural network based on the current observation.

The **Never Give UP (NGU)** [17] is a parametric exploration method that introduces episodic mechanism to intrinsically motivated rewards. Utilizing prediction errors to measure lifelong novelty, this approach also implements an episodic memory to maximize state diversity within this memory.

The **Random Encoders for Efficient Exploration (RE3)** [4, 6] APT is the first approach to propose k NN particles for state entropy maximization. It learns behaviors and representations by k NN particles and contrastive representation learning, respectively. RE3 replaces the contrastive representation learning

process with a random encoder to avoid pre-training for representation.

The **Rényi State Entropy Maximization (RISE)** [7] is a combination of RE3 and Rényi entropy. It replaces Shannon entropy with Rényi entropy and incorporates autoencoders and K-NN methods to estimate entropy in the latent space. RISE emphasizes learning acceleration by leveraging both extrinsic and intrinsic rewards. However, in our experiment, we solely utilize intrinsic rewards.

PROOFS

The Proof is highly inspired by and based on works for trajectory-wise reward redistribution [31, 32].

Proof.

$$\begin{aligned} \text{let } A &= \left(H_{\mathbf{s} \in \tau}(\mathbf{s}) - \left[\sum_{t=0}^{T_\tau-1} r_{ep}(\mathbf{s}_{t+1}) \right] \right), \\ \Rightarrow \mathbb{E}_{\tau \in D} [\mathbb{E}_{t \sim \mathbb{U}}(A^2)] &= \mathcal{L}(r_{ep}). \\ \text{let } B &= \left(\left[\sum_{t=0}^{T_\tau-1} r_{ep}(\mathbf{s}_{t+1}) \right] - T_\tau \cdot r_{ep}(\mathbf{s}_{t+1}) \right), \\ \Rightarrow \mathbb{E}_{t \sim \mathbb{U}}(B) &= 0. \end{aligned} \quad (16)$$

where $t \sim \mathbb{U}$ refers to a single time index t that is uniformly sampled from an interval $[0, T_\tau - 1]$.

$$\begin{aligned} \tilde{\mathcal{L}}(r_{ep}) &= \mathcal{L}(r_{ep}) + \mathbb{E}_{\tau \in D} [T_\tau^2 \cdot V_{\mathbf{s} \in \tau}(r_{ep}(\mathbf{s}))], \\ &= \mathcal{L}(\hat{r}) + \mathbb{E}_{\tau \in D} [\mathbb{E}_{t \sim \mathbb{U}} B^2], \\ &= \mathbb{E}_{\tau \in D} [\mathbb{E}_{t \sim \mathbb{U}} A^2] + 2\mathbb{E}_{\tau \in D} [A \mathbb{E}_{t \sim \mathbb{U}}(B)] + \mathbb{E}_{\tau \in D} [\mathbb{E}_{t \sim \mathbb{U}} B^2], \\ &= \mathbb{E}_{\tau \in D} [\mathbb{E}_{t \sim \mathbb{U}} (A^2 + 2AB + B^2)], \\ &= \mathbb{E}_{\tau \in D} [\mathbb{E}_{t \sim \mathbb{U}} (H_{\mathbf{s} \in \tau}(\mathbf{s}) \\ &\quad - \left[\sum_{t=0}^{T_\tau-1} r_{ep}(\mathbf{s}_{t+1}) \right] + \left[\sum_{t=0}^{T_\tau-1} r_{ep}(\mathbf{s}_{t+1}) \right] - T_\tau \cdot r_{ep}(\mathbf{s}_{t+1}))^2], \\ &= \mathbb{E}_{\tau \in D} [\mathbb{E}_{t \sim \mathbb{U}} (H_{\mathbf{s} \in \tau}(\mathbf{s}) - T_\tau \cdot r_{ep}(\mathbf{s}_{t+1}))^2] \end{aligned} \quad (17)$$

This scenario represents a classic mean square error (MSE) minimization problem, and its solution can be formulated as follows:

$$\begin{aligned} r_{ep}^*(\mathbf{s}_{t+1}) &= \underset{r_{ep}(\mathbf{s}_{t+1})}{\operatorname{argmin}} \left[\mathbb{E}_{\tau \in D} [(H_{\mathbf{s} \in \tau}(\mathbf{s}) - T_\tau \cdot r_{ep}(\mathbf{s}_{t+1}))^2 \cdot \mathbb{I}(\mathbf{s}_{t+1}, \tau)] \right] \\ &= \left\{ r_{ep}(\mathbf{s}_{t+1}) \left| \frac{\mathbb{d} [\mathbb{E}_{\tau \in D} [(H_{\mathbf{s} \in \tau}(\mathbf{s}) - T_\tau \cdot r_{ep}(\mathbf{s}_{t+1}))^2 \cdot \mathbb{I}(\mathbf{s}_{t+1}, \tau)]]}{\mathbb{d}[r_{ep}(\mathbf{s}_{t+1})]} = 0 \right. \right\} \\ &= \mathbb{E}_{\tau \sim D} \left[\frac{H_{\mathbf{s} \in \tau}(\mathbf{s})}{T_\tau} \cdot \mathbb{I}(\mathbf{s}_{t+1}, \tau) \right] \end{aligned} \quad (18)$$

Here we fix the T_τ as a constant. If we consider a changing T_τ , the optimal solution here will become $\frac{\sum_{\tau \in D} T_\tau H_{\mathbf{s} \in \tau}(\mathbf{s}) \mathbb{I}(\mathbf{s}_{t+1}, \tau)}{\sum_{\tau \in D} T_\tau^2 \mathbb{I}(\mathbf{s}_{t+1}, \tau)}$.

1) *Proof of Proposition 2:*

a) *The Gaussian kernel density estimation entropy estimator::* H_{KDE} with the set of visited states $\{\mathbf{s}_i\}_{i=1}^N$ is given by:

$$\begin{aligned} H_{\text{KDE}}(\mathbf{s}) &= -\frac{1}{N} \sum_{i=1}^N \log \left[\frac{1}{N} \sum_{j=1}^N \kappa(\mathbf{s}_i, \mathbf{s}_j) \right], \\ &= \frac{1}{N} \sum_{i=1}^N -\log \left(\frac{1}{N} \sum_{j=1}^N (e^{-\frac{\|\mathbf{s}_i - \mathbf{s}_j\|_2^2}{2\sigma}}) \right), \\ &\propto \frac{1}{N} \sum_{i=1}^N -\log \left(\sum_{j=1}^N (e^{-\frac{\|\mathbf{s}_i - \mathbf{s}_j\|_2^2}{2\sigma}}) \right) \end{aligned} \quad (19)$$

We now find the condition for $\sum_{j=1}^N (e^{-\frac{\|\mathbf{s} - \mathbf{s}_j\|_2^2}{2\sigma}}) = \sum_{j \in k\text{NN}} (e^{-\frac{\|\mathbf{s} - \mathbf{s}_j\|_2^2}{2\sigma}})$. For a certain \mathbf{s} , we re-sort $\{\mathbf{s}_i\}_{i=1}^N$ in ascending order according to pair-wise distances for \mathbf{s} , such that:

$$\sum_{j=1}^N (e^{-\frac{\|\mathbf{s} - \mathbf{s}_j\|_2^2}{2\sigma}}) = \sum_{j \in k\text{NN}} (e^{-\frac{\|\mathbf{s} - \mathbf{s}_j\|_2^2}{2\sigma}}) + \sum_{j=k+1}^N (e^{-\frac{\|\mathbf{s} - \mathbf{s}_j\|_2^2}{2\sigma}}) \quad (20)$$

Given the tolerance ϵ , we have the condition:

$$\begin{aligned} \sum_{j=k+1}^N (e^{-\frac{\|\mathbf{s} - \mathbf{s}_j\|_2^2}{2\sigma}}) &< \epsilon, \\ \Rightarrow \sum_{j=k+1}^N (e^{-\frac{\|\mathbf{s} - \mathbf{s}_j\|_2^2}{2\sigma}}) &\leq (N-k) e^{-\frac{\|\mathbf{s} - \mathbf{s}_k\|_2^2}{2\sigma}} < \epsilon, \\ \Rightarrow \|\mathbf{s} - \mathbf{s}_k\| &> [2\sigma \log \frac{N-k}{\epsilon}]^{\frac{1}{2}}, \\ \Rightarrow \forall \mathbf{s}, \max [\|\mathbf{s} - \mathbf{s}_j\|_{j \in k\text{NN}}] &> [2\sigma \log \frac{N-k}{\epsilon}]^{\frac{1}{2}} \end{aligned} \quad (21)$$

b) *The 2nd-order Matrix-based Rényi estimator::* H_2 with the set of visited states $\{\mathbf{s}_i\}_{i=1}^N$ is given by:

$$H_2(\mathbf{s}) = \frac{1}{1-2} \log[\operatorname{tr}(\hat{A}^2)] \quad (22)$$

where “tr” is the matrix trace, $\hat{A} = K / \operatorname{tr}(K)$ is the trace normalized K , $\lambda_n(\hat{A})$ denotes the n -th eigenvalue of \hat{A} . Given the definition of Gram matrix, we have:

$$\begin{aligned} H_2(\mathbf{s}) &= -\frac{1}{2} \log \left[\sum_{i=1}^N \sum_{j=1}^N \kappa(\mathbf{s}_i, \mathbf{s}_j)^2 \right] \\ &\propto \frac{1}{N} \log \sum_{i=1}^N - \left(\sum_{j=1}^N (e^{-\frac{\|\mathbf{s}_i - \mathbf{s}_j\|_2^2}{2\sigma}}) \right) \\ &= \frac{1}{N} \log \sum_{i=1}^N r_i(\mathbf{s}) \end{aligned} \quad (23)$$

We see here that a minor difference to KDE lies in the reversed order of occurrence of the logarithm. Therefore, the condition for $\sum_{j=1}^N (e^{-\frac{\|\mathbf{s} - \mathbf{s}_j\|_2^2}{2\sigma}}) = \sum_{j \in k\text{NN}} (e^{-\frac{\|\mathbf{s} - \mathbf{s}_j\|_2^2}{2\sigma}})$ is same to KDE.

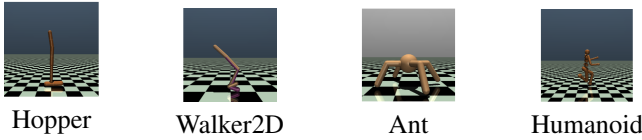


Fig. 11: Visual interfaces of robotic environments



Fig. 12: The map of Stage 1-1 in the Mario game.

DETAILS OF EXPERIMENTAL SETTING

All experiments are conducted on single V-100 GPUs, where the maximum memory usage is up to 10G for each single training process.

Experiments are mainly validated in the following five environments:

Hopper is a two-dimensional, one-legged agent composed of four main body parts: the torso at the top, the thigh in the middle, the leg at the bottom, and a single foot serving as the base. The observation is a 11D vector.

Walker2D is a classical deterministic control environment where a car is placed randomly at the bottom of a sinusoidal valley. The available actions for the car are limited to accelerations in either direction. The observation is a 17D vector.

Ant is a three-dimensional robot composed of a single torso, which is a freely rotating body, and four legs connected to it. Each leg consists of two links. The observation is a 27D vector.

Humanoid The 3D bipedal robot is designed to simulate a human. It has a torso (abdomen) with a pair of legs and arms. The legs each consist of three body parts, and the arms 2 body parts (representing the knees and elbows respectively). The observation is a 376D vector.

Mario is a classical 2D video game where Mario is placed at the starting point (leftmost). The Mario has 16 available actions, allowing it to move in all directions. We select the Stage 1-1 for our experiments.

In our experiments, we adopt fixed neural encoders $f(o)$ to map raw observations to state space for entropy estimation. For Mujoco environment, they are fully-connected random deep neural networks with 2 hidden layers and 64 neurons in each hidden layer. The observation are encoded to 5D vectors. Then we append these vectors to spatial coordinates and torso orientations. State entropy is maximized over spaces of these concatenated representations.

For Mario, we pre-train an encoder with random policy using Spatiotemporal Deep Infomax [30], a contrastive state representation learning method that maximizes the mutual information across both the spatial and temporal axes. Hyper-parameter selection is given in Table II

The encoder maps frames of the Mario game to a 32D representation space. State entropy is maximized over spaces of these 32D vectors.

Hyper-Parameter Setting of ELEMENT in all five environments are given by Table III, IV, V, VI. In Mujoco

Hyper-parameters	Value
number of steps	5e+6
nNum-processes	8
lr	3e-4
batch-size	64
use_multiple_predictors	False
fatience	15
feature-size	32
entropy-threshold	0.6
layer_num	2
activation_function	relu
last_activation	None
collect-mode	random_agent

TABLE II: Hyper-parameters of Spatiotemporal Deep Infomax

Hyper-parameters	Value
β	0.5
estimator	KDE
σ	1
T_τ	1000
graph_search_step	20
num_graph_search_initial	20
graph_update_depth	2
k_{lifelong}	3
U	5e+5
T_u	5e+4

TABLE III: Hyper-parameters of ELEMENT on Hopper

Hyper-parameters	Value
β	0.5
estimator	k NN
$k_{\text{estimator}}$	5
T_τ	1000
graph_search_step	10
num_graph_search_initial	5
graph_update_depth	2
k_{lifelong}	3
U	5e+5
T_u	5e+4

TABLE IV: Hyper-parameters of ELEMENT on Walker2D

Hyper-parameters	Value
β	0.5
estimator	Matrix-based Rényi
σ	1
α	3
T_τ	1000
graph_search_step	20
num_graph_search_initial	10
graph_update_depth	2
k_{lifelong}	3
U	5e+5
T_u	5e+4

TABLE V: Hyper-parameters of ELEMENT on Ant

Hyper-parameters	Value
β	0.5
estimator	Matrix-based Rényi
σ	1
α	3
T_τ	1000
graph_search_step	20
num_graph_search_initial	10
graph_update_depth	2
k_{lifelong}	3
U	5e+5
T_u	5e+4

TABLE VI: Hyper-parameters of ELEMENT on Humanoid

environments, we adopt SAC as backbones. For the SAC³ oracle, we summarize our hyper-parameters in Table VII.

Hyper-parameters	Value
initial temperature	0.2
gamma	0.99
actor_lr	3e-4
critic_lr	3e-4
q_lr	3e-4
soft_update_rate	0.005
hidden_dim	256
memory_size	1e+6
layer_num	3
batch_size	128
layer_num	3
activation_function	torch.relu
last_activation	None

TABLE VII: Hyper-parameters of SAC

In Mario, A3C is used as backbone whose hyper-parameters are summarized in Table VIII. The neural structure is given by:

$$\begin{aligned}
self.conv1 &= nn.Conv2d(1, 32, 3, stride = 2, padding = 1) \\
self.conv2 &= nn.Conv2d(32, 32, 3, stride = 2, padding = 1) \\
self.conv3 &= nn.Conv2d(32, 32, 3, stride = 2, padding = 1) \\
self.conv4 &= nn.Conv2d(32, 32, 3, stride = 2, padding = 1) \\
self.lstm &= nn.LSTMCell(32 * 6 * 6, 512) \\
self.critic_linear &= nn.Linear(512, 1) \\
self.actor_linear &= nn.Linear(512, 16)
\end{aligned}
\tag{24}$$

Hyper-parameters	Value
action_type	complex
gamma	0.9
actor_lr	1e-4
critic_lr	1e-4
parameter for GAE	1.0
entropy coefficient	0.01
num_local_steps	300
num_processes	6
activation_function	torch.relu
last_activation	None

TABLE VIII: Hyper-parameters of A3C

REFERENCES

- [1] V. Mnih, K. Kavukcuoglu, D. Silver, A. A. Rusu, J. Veness, M. G. Bellemare, A. Graves, M. Riedmiller, A. K. Fidjeland, G. Ostrovski *et al.*, “Human-level control through deep reinforcement learning,” *nature*, vol. 518, no. 7540, pp. 529–533, 2015.
- [2] D. Silver, A. Huang, C. J. Maddison, A. Guez, L. Sifre, G. Van Den Driessche, J. Schrittwieser, I. Antonoglou, V. Panneershelvam, M. Lanctot *et al.*, “Mastering the game of go with deep neural networks and tree search,” *nature*, vol. 529, no. 7587, pp. 484–489, 2016.
- [3] S. Amin, M. Gomrokchi, H. Satija, H. van Hoof, and D. Precup, “A survey of exploration methods in reinforcement learning,” *arXiv preprint arXiv:2109.00157*, 2021.
- [4] H. Liu and P. Abbeel, “Behavior from the void: Unsupervised active pre-training,” *Advances in Neural Information Processing Systems*, vol. 34, pp. 18 459–18 473, 2021.
- [5] M. Mutti, L. Pratissoli, and M. Restelli, “Task-agnostic exploration via policy gradient of a non-parametric state entropy estimate,” in *Proceedings of the AAAI Conference on Artificial Intelligence*, vol. 35, no. 10, 2021, pp. 9028–9036.
- [6] Y. Seo, L. Chen, J. Shin, H. Lee, P. Abbeel, and K. Lee, “State entropy maximization with random encoders for efficient exploration,” in *International Conference on Machine Learning*. PMLR, 2021, pp. 9443–9454.
- [7] M. Yuan, M.-O. Pun, and D. Wang, “Rényi state entropy maximization for exploration acceleration in reinforcement learning,” *IEEE Transactions on Artificial Intelligence*, 2023.
- [8] E. Hazan, S. Kakade, K. Singh, and A. Van Soest, “Provably efficient maximum entropy exploration,” in *International Conference on Machine Learning*. PMLR, 2019, pp. 2681–2691.
- [9] C. Zhang, Y. Cai, L. Huang, and J. Li, “Exploration by maximizing rényi entropy for reward-free rl framework,” in *Proceedings of the AAAI Conference on Artificial Intelligence*, vol. 35, no. 12, 2021, pp. 10 859–10 867.
- [10] A. Nedergaard and M. Cook, “k-means maximum entropy exploration,” *arXiv preprint arXiv:2205.15623*, 2022.
- [11] D. Yarats, R. Fergus, A. Lazaric, and L. Pinto, “Reinforcement learning with prototypical representations,” in *International Conference on Machine Learning*. PMLR, 2021, pp. 11 920–11 931.
- [12] D. Tiapkin, D. Belomestny, D. Calandriello, E. Moulines, R. Munos, A. Naumov, P. Perrault, Y. Tang, M. Valko, and P. Menard, “Fast rates for maximum entropy exploration,” *arXiv preprint arXiv:2303.08059*, 2023.
- [13] H. Singh, N. Misra, V. Hnizdo, A. Fedorowicz, and E. Demchuk, “Nearest neighbor estimates of entropy,” *American journal of mathematical and management sciences*, vol. 23, no. 3-4, pp. 301–321, 2003.
- [14] M. Bellemare, S. Srinivasan, G. Ostrovski, T. Schaul, D. Saxton, and R. Munos, “Unifying count-based ex-

³<https://github.com/seolhokim/Mujoco-Pytorch>

- ploration and intrinsic motivation,” *Advances in neural information processing systems*, vol. 29, 2016.
- [15] C. Stanton and J. Clune, “Deep curiosity search: Intra-life exploration can improve performance on challenging deep reinforcement learning problems,” *arXiv preprint arXiv:1806.00553*, 2018.
 - [16] A. Ecoffet, J. Huizinga, J. Lehman, K. O. Stanley, and J. Clune, “Go-explore: a new approach for hard-exploration problems,” *arXiv preprint arXiv:1901.10995*, 2019.
 - [17] A. P. Badia, P. Sprechmann, A. Vitvitskyi, D. Guo, B. Piot, S. Kapturowski, O. Tieleman, M. Arjovsky, A. Pritzel, A. Bolt *et al.*, “Never give up: Learning directed exploration strategies,” *arXiv preprint arXiv:2002.06038*, 2020.
 - [18] L. G. S. Giraldo, M. Rao, and J. C. Principe, “Measures of entropy from data using infinitely divisible kernels,” *IEEE Transactions on Information Theory*, vol. 61, no. 1, pp. 535–548, 2014.
 - [19] K. Hajebi, Y. Abbasi-Yadkori, H. Shahbazi, and H. Zhang, “Fast approximate nearest-neighbor search with k-nearest neighbor graph,” in *Twenty-Second International Joint Conference on Artificial Intelligence*, 2011.
 - [20] T. Debatty, P. Michiardi, and W. Mees, “Fast online k-nn graph building,” *arXiv preprint arXiv:1602.06819*, 2016.
 - [21] A. Rényi, “On measures of entropy and information,” in *Proceedings of the Fourth Berkeley Symposium on Mathematical Statistics and Probability, Volume 1: Contributions to the Theory of Statistics*, vol. 4. University of California Press, 1961, pp. 547–562.
 - [22] J. C. Principe, *Information theoretic learning: Renyi’s entropy and kernel perspectives*. Springer Science & Business Media, 2010.
 - [23] R. A. Davis, K.-S. Lii, and D. N. Politis, “Remarks on some nonparametric estimates of a density function,” *Selected Works of Murray Rosenblatt*, pp. 95–100, 2011.
 - [24] L. Lee, B. Eysenbach, E. Parisotto, E. Xing, S. Levine, and R. Salakhutdinov, “Efficient exploration via state marginal matching,” *arXiv preprint arXiv:1906.05274*, 2019.
 - [25] J. Schulman, S. Levine, P. Abbeel, M. Jordan, and P. Moritz, “Trust region policy optimization,” in *International conference on machine learning*. PMLR, 2015, pp. 1889–1897.
 - [26] D. Pathak, P. Agrawal, A. A. Efros, and T. Darrell, “Curiosity-driven exploration by self-supervised prediction,” in *International conference on machine learning*. PMLR, 2017, pp. 2778–2787.
 - [27] Y. Burda, H. Edwards, A. Storkey, and O. Klimov, “Exploration by random network distillation,” in *International Conference on Learning Representations*, 2019.
 - [28] E. Pfaffelhuber, “Learning and information theory,” *International journal of neuroscience*, vol. 3, no. 2, pp. 83–88, 1972.
 - [29] D. B. Lenat, *AM: an artificial intelligence approach to discovery in mathematics as heuristic search*. Stanford University, 1976.
 - [30] A. Anand, E. Racah, S. Ozair, Y. Bengio, M.-A. Côté, and R. D. Hjelm, “Unsupervised state representation learning in atari,” *Advances in neural information processing systems*, vol. 32, 2019.
 - [31] T. Gangwani, Y. Zhou, and J. Peng, “Learning guidance rewards with trajectory-space smoothing,” *Advances in Neural Information Processing Systems*, vol. 33, pp. 822–832, 2020.
 - [32] Z. Ren, R. Guo, Y. Zhou, and J. Peng, “Learning long-term reward redistribution via randomized return decomposition,” *arXiv preprint arXiv:2111.13485*, 2021.
 - [33] Y. Efroni, N. Merlis, and S. Mannor, “Reinforcement learning with trajectory feedback,” in *Proceedings of the AAAI conference on artificial intelligence*, vol. 35, no. 8, 2021, pp. 7288–7295.
 - [34] T. Haarnoja, A. Zhou, K. Hartikainen, G. Tucker, S. Ha, J. Tan, V. Kumar, H. Zhu, A. Gupta, P. Abbeel *et al.*, “Soft actor-critic algorithms and applications,” *arXiv preprint arXiv:1812.05905*, 2018.
 - [35] V. Mnih, A. P. Badia, M. Mirza, A. Graves, T. Lillicrap, T. Harley, D. Silver, and K. Kavukcuoglu, “Asynchronous methods for deep reinforcement learning,” in *International conference on machine learning*. PMLR, 2016, pp. 1928–1937.
 - [36] G. Brockman, V. Cheung, L. Pettersson, J. Schneider, J. Schulman, J. Tang, and W. Zaremba, “Openai gym,” 2016.
 - [37] S. Levine, A. Kumar, G. Tucker, and J. Fu, “Offline reinforcement learning: Tutorial, review, and perspectives on open problems,” *arXiv preprint arXiv:2005.01643*, 2020.
 - [38] C. Jin, A. Krishnamurthy, M. Simchowitz, and T. Yu, “Reward-free exploration for reinforcement learning,” in *International Conference on Machine Learning*. PMLR, 2020, pp. 4870–4879.
 - [39] A. Kumar, A. Zhou, G. Tucker, and S. Levine, “Conservative q-learning for offline reinforcement learning,” *Advances in Neural Information Processing Systems*, vol. 33, pp. 1179–1191, 2020.
 - [40] F. Torabi, G. Warnell, and P. Stone, “Behavioral cloning from observation,” *arXiv preprint arXiv:1805.01954*, 2018.